CORE
Metadata, citation and similar papers at core.ac.uk
Provided by Elsevier - Publisher Connector
Cell, Vol. 119, 777–788, December 17, 2004, Copyright ©2004 by Cell Press

Recruitment of the INO80 Complex by H2A Phosphorylation Links ATP-Dependent Chromatin Remodeling with DNA Double-Strand Break Repair

Haico van Attikum,[1,3] Olivier Fritsch,[2] Barbara Hohn,[2] and Susan M. Gasser[1,3,*]
[1]University of Geneva
Department of Molecular Biology and
NCCR Frontiers in Genetics Program
Quai Ernest Ansermet 30
CH-1211 Geneva 4
Switzerland
[2]Friedrich Miescher Institute
for Biomedical Research
Maulbeerstrasse 66
4058 Basel
Switzerland

Summary

The budding yeast INO80 complex is a conserved ATP-dependent nucleosome remodeler containing actin-related proteins Arp5 and Arp8. Strains lacking *INO80*, *ARP5*, or *ARP8* have defects in transcription. Here we show that these mutants are hypersensitive to DNA damaging agents and to double-strand breaks (DSBs) induced by the HO endonuclease. The checkpoint response and most transcriptional modulation associated with induction of DNA damage are unaffected by these mutations. Using chromatin immunoprecipitation we show that Ino80, Arp5, and Arp8 are recruited to an HO-induced DSB, where a phosphorylated form of H2A accumulates. Recruitment of Ino80 is compromised in cells lacking the H2A phosphoacceptor S129. Finally, we demonstrate that conversion of the DSB into ssDNA is compromised in *arp8* and H2A mutants, which are both deficient for INO80 activity at the site of damage. These results implicate INO80-mediated chromatin remodeling directly at DSBs, where it appears to facilitate processing of the lesion.

Introduction

Chromosomal double-strand breaks (DSBs) are induced by a variety of agents, including ionizing radiation and radiomimetic drugs. Strand breaks also arise as aberrant by-products of DNA replication, particularly when template DNA has been alkylated by methyl methanesulfonate (MMS). Inefficient or inaccurate repair of double-strand breaks contributes to genomic instability and to tumorigenesis or cell death in mammals (Zhou and Elledge, 2000). The packaging of eukaryotic genomes into nucleosomes reduces access to sites of damage, impairing not only the detection of lesions but also their repair.

Eukaryotes have two classes of enzymes that help overcome the barrier imposed by chromatin structure. The first class regulates access through the covalent addition or removal of posttranslational modifications of histone tails (e.g., serine phosphorylation or lysine acetylation), while the second class contains large ATP-dependent complexes that remodel nucleosomes (Lusser and Kadonaga, 2003; Peterson and Cote, 2004). One of the earliest events that correlates with the repair response to DSBs and other damage is the phosphorylation of the C-terminal tail of histone H2A in yeast, or of H2A-X in higher eukaryotes by ATM/ATR-like kinases (Downs et al., 2000; Fernandez-Capetillo et al., 2004; Nakamura et al., 2004). In addition, both the acetylation and deacetylation of the N-terminal tail of histone H4 by the NuA4 HAT and Sin3/Rpd3 HDAC complexes contribute to efficient DSB repair (Bird et al., 2002; Jazayeri et al., 2004). Although it has been proposed that nucleosome remodeling facilitates access to chromatin for enzymes involved in repair, no member of the SNF2/SWI2 family of ATPases has been directly implicated in this process, apart from Rad54, which specifically promotes Rad51-mediated strand exchange during recombination (Jaskelioff et al., 2003; Petukhova et al., 1998).

A conserved member of the SWI/SNF family, the Ino80 ATPase, was recently identified in budding yeast (Ebbert et al., 1999; Shen et al., 2000). The purified Ino80 complex (INO80) contains about 12 polypeptides, possesses 3′–5′ helicase activity, and remodels chromatin by shifting nucleosomes. Among its subunits are two homologs of the bacterial RuvB protein, Rvb1 and Rvb2, and three actin-related proteins, Arp4, Arp5, and Arp8, two of which are implicated in histone binding (Harata et al., 1999; Shen et al., 2003). Strains lacking *INO80* not only have misregulated transcription but also are hypersensitive to DNA-damaging agents (Mizuguchi et al., 2004; Shen et al., 2000), suggesting that chromatin remodeling driven by the INO80 complex may not only regulate RNA pol II promoters, but may facilitate DNA repair as well. Here we test this hypothesis by examining the role of the INO80 complex in DSB repair.

Results

Arp5 and Arp8, Like Ino80, Are Implicated in Multiple Pathways of DSB Repair

In eukaryotes, two major pathways exist for the repair of DSBs. Homologous recombination (HR) relies on the transfer of genetic information of a homologous daughter molecule to the site of damage, while nonhomologous end joining (NHEJ) mediates DNA end ligation without recombination or sequence homology requirements. The first step in our study was to investigate in more detail the phenotypes of *ino80*, *arp5*, and *arp8* mutants. The two actin-related subunits, Arp5 and Arp8, are required for INO80-dependent chromatin remodeling activity (Shen et al., 2003), yet unlike deletions of *INO80*, which encodes the ATPase itself, complete *ARP5* and *ARP8* deletions are not lethal in most commonly used yeast backgrounds. Given this variation, we chose a background that could tolerate the deletion of *INO80*, *ARP5*, or *ARP8* and tested the sensitivity of each mutant

*Correspondence: susan.gasser@fmi.ch
[3]Present Address: Friedrich Miescher Institute for Biomedical Research, Maulbeerstrasse 66, 4058 Basel, Switzerland.

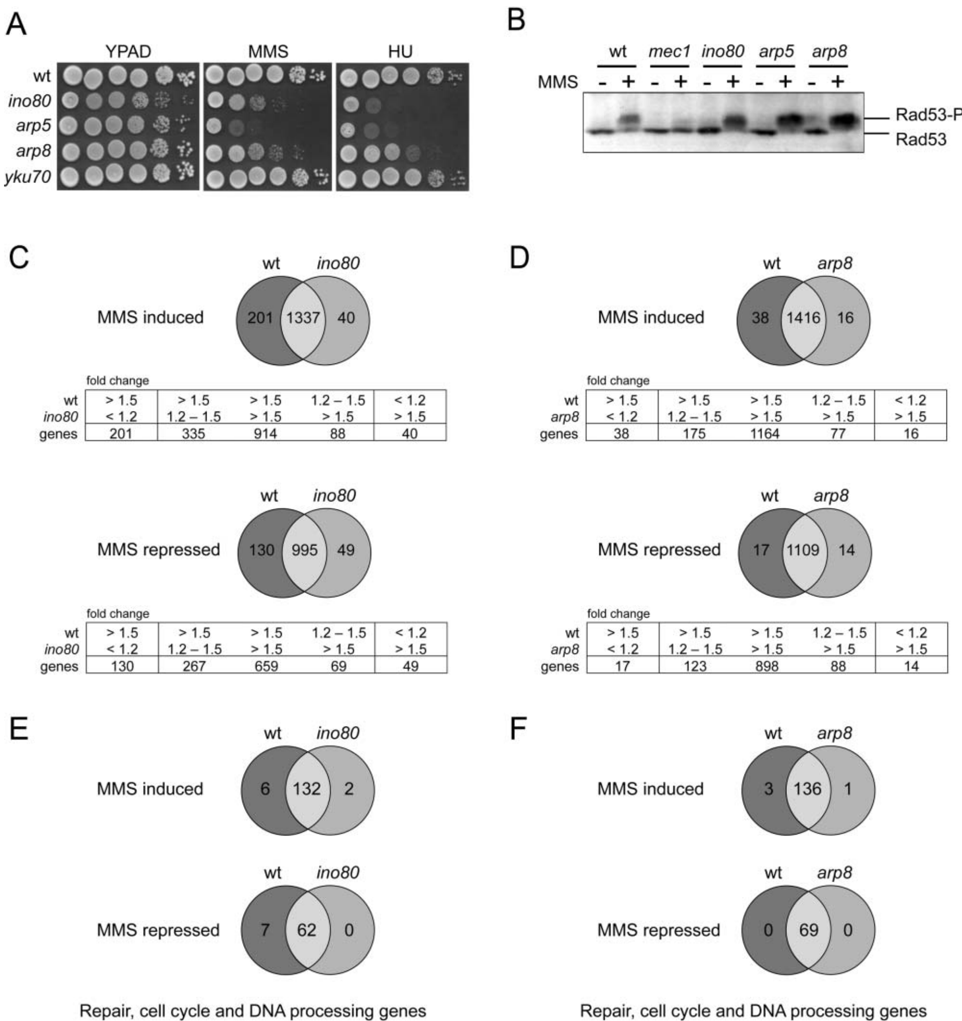

Figure 1. INO80 Mutations Affect Survival but Not Checkpoint Response on MMS

(A) Strains deficient for *INO80, ARP5*, and *ARP8* are hypersensitive to DNA damage. Survival of the indicated isogenic yeast strains in the S288C background was determined by plating serial 10-fold dilutions on nonselective medium containing 0.03% methyl methanesulfonate (MMS) or 100 mM hydroxyurea (HU). Growth was monitored after 4–5 days at 30°C.

(B) Activation of the central checkpoint kinase Rad53 is normal in *ino80, arp5*, and *arp8* cells. A polyclonal antibody against Rad53 detects the kinase and its hyperphosphorylated form (Rad53-P) in whole-cell extracts from wild-type, *mec1, ino80, arp5*, and *arp8* cells treated or not with 0.05% MMS for 2 hr.

(C) Venn diagram showing the number of genes whose expression levels were changed significantly in response to MMS treatment (0.1%) in isogenic *ino80* and wild-type strains. The overlap represents commonly regulated genes. The table below shows the fold change in expression levels for differentially and commonly regulated genes. Specific genes are listed in Supplemental Table S3 on the *Cell* website.

(D) As (C), but for isogenic *arp8* and wild-type strains.

(E) Venn diagrams showing the number of genes, known as repair, cell cycle, or DNA processing genes, whose expression was significantly changed (>1.5-fold induced or repressed) in response to MMS treatment in *ino80* mutant versus wild-type. The overlap represents commonly regulated genes. Specific genes are mentioned in the text and in Supplemental Tables S2 and S4 on the *Cell* website.

(F) As (E), but for isogenic *arp8* and wild-type strains. Genes misregulated in the *arp8* mutant are generally a subset of those misregulated in *ino80* cells. Specific genes are mentioned in the text and in Supplemental Table S4 and are summarized in Supplemental Table S2 on the *Cell* website.

to the alkylating agent MMS, which induces both single- and double-strand breaks during DNA replication, and to hydroxyurea (HU), which depletes dNTP pools and activates the intra-S checkpoint (Figure 1A). Deletion of any of these core INO80 subunits renders cells hypersensitive to growth in the presence of either MMS or HU. The pattern of sensitivity of *arp5*, *arp8*, and *ino80* mutants thus more closely resembles that of strains deficient in HR, such as *rad52*, than a strain lacking *YKU70*, which is deficient for NHEJ (Figure 1A; Table 1). Hypersensitivity to DNA-damaging agents may indicate that repair is compromised, yet could also stem from impaired checkpoint activation and/or altered gene expression in response to genetic insult.

To assess the efficiency of checkpoint activation in *ino80*, *arp5*, and *arp8* mutants, we monitored the phosphorylation status of the central checkpoint kinase Rad53. Rad53 phosphorylation depends on the activity of the ATR-like kinase Mec1 (Melo and Toczyski, 2002), and a large Mec1-dependent mobility shift reflecting Rad53 phosphorylation occurs upon exposure to MMS in wild-type cells (Figure 1B). In *ino80*, *arp5*, and *arp8* mutants, the Rad53 phosphorylation level is the same, if not higher, than that found in wild-type cells under identical conditions. This activation and the subsequent induction of *RNR3* by MMS (see below), indicate that the checkpoint response is intact in the absence of INO80, making it unlikely that checkpoint defects account for the mutants' sensitivity to MMS.

To examine whether INO80 affects repair indirectly by regulating gene transcription, we first compared the global expression pattern of wild-type and *ino80* and wild-type and *arp8* mutant strains in the absence of MMS. In *ino80* cells, we find 1156 genes (i.e., 647 more than reported in Mizuguchi et al., 2004) either induced or repressed by at least 1.5-fold (Supplemental Table S1 at http://www.cell.com/cgi/content/full/119/6/777/DC1/). With respect to global expression patterns, far fewer genes are induced or repressed significantly in *arp8* cells (395 genes have >1.5-fold variation; Supplemental Table S1 on the *Cell* website). Importantly, no genes that are directly implicated in DNA repair or in the checkpoint response were repressed in both mutants, and only four such genes were coordinately induced. These genes are *NHP10* and *IES1*, which encode subunits of the INO80 complex itself (Shen et al., 2003), and *RAD2* and *RAD28*, which encode proteins involved in UV-induced NER (Reagan and Friedberg, 1997). Among the transcripts whose levels drop in the *ino80*-deficient strain (and not in *arp8)*, we find *RAD23*, *MSH6*, and *RAD5*, which regulate NER, mismatch repair, and postreplication repair, respectively, *ARP4*, a component of several chromatin remodeling complexes, and several factors associated with the replication fork (Mrc1, Tof1, Rfc1, and the Cdc9 ligase, see Supplemental Table S2 on the *Cell* website).

An analogous transcriptome analysis was performed after 1 hr exposure to MMS in the wild-type and mutant cells. The expression level of >2500 mRNAs was altered (induced or repressed) by at least 1.5-fold (Figures 1C and 1D), and among these genes the vast majority respond indistinguishably in wild-type, *ino80* and *arp8* strains. Globally, 96% of those modulated in the *ino80* mutant and 99% in the *arp8* mutant are the same as in wild-type cells, while 88% and 98% of the genes that respond in wild-type cells respond similarly in *ino80* and *arp8* cells, respectively (Figures 1C and 1D and Supplemental Table S3 on the *Cell* website). Although a significant number of genes (334) have the same modulation in *arp8* and wild-type cells, but not in the strain lacking Ino80, the vast majority of these genes have no connection with either the DNA repair machinery or the damage response (Jelinsky and Samson, 1999).

In order to focus on genes relevant for cell survival, we monitored MMS-induced changes for 702 genes encoding repair, DNA processing, or cell cycle regulatory proteins as designated by the comprehensive yeast genome database (MIPS; www.mips.gsf.de) and the *Saccharomyces* genome database (SGD; www.yeastgenome.org; see Supplemental Table S4 on the *Cell* website). Repair and checkpoint-regulated genes such as *RAD51*, *YKU70*, and *RNR3* were indeed induced by 1hr exposure to MMS, as were 8 of the 12 subunits of the INO80 complex. Their induction showed no requirement for INO80, being identical in wild-type and the two mutant strains (see Supplemental Table S4 on the *Cell* website and data not shown). In general, among these 702 genes only six were induced in wild-type, but not *ino80* cells, while nine fail to be repressed in the *ino80* mutant (Supplemental Table S2 on the *Cell* website). Only three of these genes shared a similar pattern of misregulation in the *arp8* strain (Figures 1E and 1F and Supplemental Table S2 on the *Cell* website), and of these, two have no obvious link to DNA repair (*FIN1* and *MKK1*, Supplemental Table

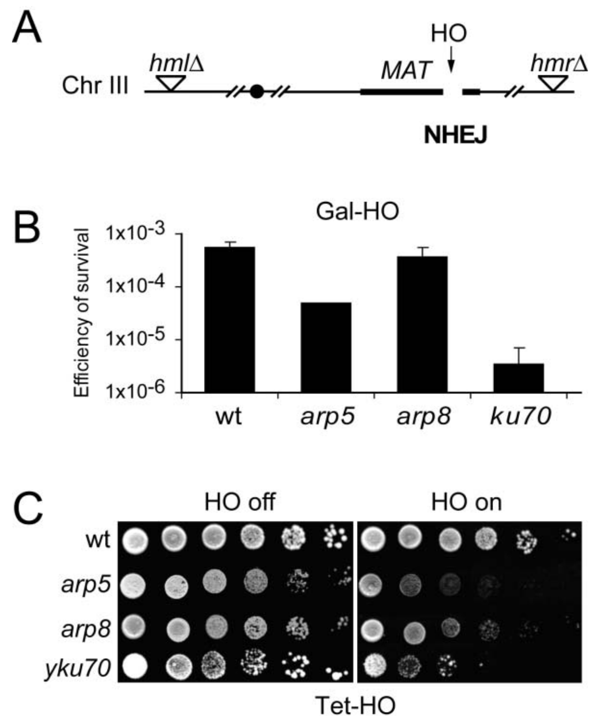

Figure 2. Mutants Lacking a Functional INO80 Complex Are Hypersensitive to DSB Induction

(A) Schematic representation of the features of Chr III in JKM179, a haploid yeast strain that contains a galactose-inducible HO endonuclease integrated at the *ADE3* locus. Upon switch to galactose, HO endonuclease is expressed, inducing a DSB at the *MAT* locus. The *HM* donor loci *HML* and *HMR* were deleted, which prevents repair of the DSB by homologous recombination. Repair can occur through NHEJ until extensive processing prevents cleavage and religation.

(B) *arp5* mutants are sensitive to the induction of a single chromosomal DSB when the HO endonuclease is expressed from a galactose-inducible promoter. Survival of indicated, isogenic strains in the JKM179 background was determined by the ratio of the numbers of colonies formed on medium containing galactose versus glucose.

(C) *arp5* and *arp8* mutants, like a *yku70* mutant, are sensitive to the induction of a single DSB induced by a tetracycline-regulated HO endonuclease. Survival of the indicated strains was determined after plating serial 10-fold dilutions on selective medium with doxycycline (HO off) and without doxycycline (HO on).

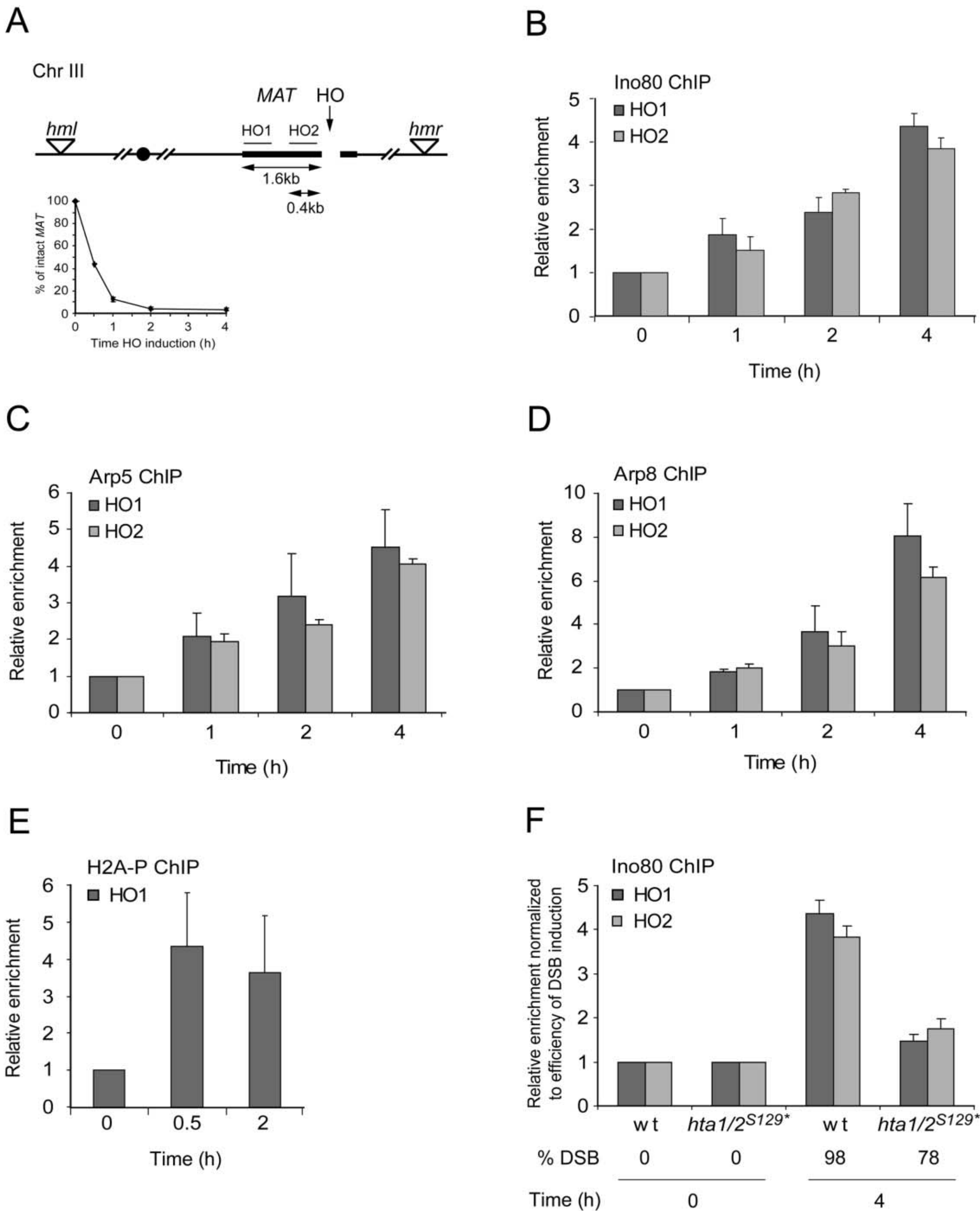

Figure 3. INO80 Recruitment to a DSB Requires H2A Phosphorylation

(A) Schematic representation of the features of Chr III (upper panel) in the haploid yeast strain that expresses the galactose-inducible HO endonuclease and bears deletions for *HML* and *HMR* loci. The primer/probe sets at HO1 and HO2 indicated. These amplify different regions near the HO DSB by quantitative real-time PCR in chromatin immunoprecipitation (ChIP) experiments. Efficiency of DSB formation at the *MAT* locus (lower panel). PCR was performed on input DNA from ChIP experiments using primers that span the HO cleavage site and primers that anneal to the *SMC2* control locus on Chr VI. Appearance of the DSB is detected by loss of the product generated by the HO primers. PCR products were quantified and the cleavage efficiency calculated as the ratio of HO/SMC signal in induced cells normalized to that of uninduced cells.

(B) Ino80 is recruited to a DSB at *MAT*. Shown is the relative fold enrichment of Ino80 at HO1 and HO2 0, 1, 2, and 4 hr after HO induction as the mean ± SD from multiple independent experiments, calculated as described in the Experimental Procedures. The signal at time 0, just prior to induction, is arbitrarily set as 1 for each condition.

(C) Arp5 is recruited to a DSB at *MAT*. Relative fold enrichment of Arp5 at HO1 and HO2 0, 1, 2, and 4 hr after HO induction is shown.

(D) Arp8 is recruited to a DSB at *MAT*. Relative fold enrichment of Arp8 at HO1 and HO2 0, 1, 2, and 4 hr after DSB induction is shown.

(E) Histone H2A at *MAT* becomes phosphorylated in response to the induction of a DSB. Relative fold enrichment of phosphorylated histone H2A at HO1 0, 0.5, and 2 hr after HO induction is shown. HO2 values were slightly lower (data not shown), consistent with observations of

S2 on the *Cell* website). The third, however, encodes DNA ligase 4, an enzyme specific for NHEJ (Schar et al., 1997; Teo and Jackson, 1997). Moreover, the regulatory partner of ligase 4, *NEJ1* (Frank-Vaillant and Marcand, 2001; Kegel et al., 2001; Valencia et al., 2001), is induced by MMS in wild-type and *arp8* cells, but not in the *ino80* strain. Since the loss of NHEJ through *YKU70* deletion has no impact on MMS survival (Figure 1A), it is unlikely that *DNL4* misregulation is directly responsible for the observed MMS sensitivity. Nonetheless, this result underscores an intriguing regulatory link between INO80 and the NHEJ pathway of DSB repair.

As mentioned above, several relevant cell cycle genes either show constitutively lower expression in the *ino80* mutant or fail to be induced by MMS in *ino80* cells but behave normally in *arp8* cells. Among these genes are *MRC1* and *TOF1*, which encode factors that influence the stability of replication forks upon HU arrest (Katou et al., 2003; Foss, 2001; Supplemental Table S2 on the *Cell* website). Although their deregulation is generally only 2-fold, we do not rule out that these lower expression levels contribute to the enhanced MMS sensitivity that we monitor for *ino80* versus *arp8* cells. The differences noted between *ino80* and *arp8* mutants further suggest that either Ino80 has functions beyond its nucleosome remodeling activity, or the Arp8-depleted INO80 complex has some residual transactivation activity in vivo (Shen et al., 2003).

Cells Lacking a Functional INO80 Complex Are Compromised for NHEJ

Based on the transcriptome analysis, INO80 does not appear to regulate HR on a transcriptional level, but there are suggestive links to NHEJ. We therefore tested whether INO80 influences the efficiency of DSB repair by NHEJ. Using a well-characterized galactose-inducible HO endonuclease system, we induced a single chromosomal DSB at the *MAT* locus, in a strain background that precludes repair by HR due to the deletion of the homologous donor loci, *HML* and *HMR* (Lee et al., 1998). Continuous expression of HO leads to cycles of cleavage and ligation until processing of the cleaved ends occurs. If cells are competent for error-prone repair by NHEJ, they will be able to grow in the presence of induced HO endonuclease, while cells deficient for NHEJ die. We demonstrate a significant drop in survival for the *yku70* deletion strain in Figure 2B, as well as for *arp5*, but not *arp8*, cells.

Because it was reported that maximal expression from galactose-inducible promoters requires a functional INO80 complex (Ebbert et al., 1999), we developed an alternative inducible HO endonuclease system, where expression is controlled by a heterologous tetracycline-regulated promoter. Continuous HO expression from this promoter again leads to lethality in the NHEJ-deficient *yku70* strain, but not in NHEJ-proficient wild-type cells (Figure 2C). In this case, with the INO80-independent induction system, both the *arp5* and *arp8* mutants show sensitivity to DSB induction, in contrast to wild-type cells. Indeed, *arp5* cells are nearly as sensitive as the *yku70* deletion strain (Figure 2C). Given that the deletion of *ino80* in either strain background is lethal, and that Arp5 and Arp8 are specific subunits of the INO80 complex (Shen et al., 2003), our results suggest that the nucleosome remodeling activity of the INO80 complex contributes to DSB repair, potentially acting both at a transcriptional level and directly at the site of damage.

Ino80, Arp5, and Arp8 Bind Near Sites of DNA Damage

To test whether INO80 functions directly in the repair of DNA damage, we probed its presence near a DSB. The association of a protein complex with a cut site can be demonstrated by chromatin immunoprecipitation (ChIP) if the position of the damage is precisely defined. This is the case with HO endonuclease-induced cleavage since the HO enzyme has a unique recognition motif found within the *MAT* locus on yeast Chr III (Figure 3A). Again, the absence of the homologous *HMR* and *HML* loci and the continuous induction of the HO endonuclease ensure that the DSB persists, allowing an immunobiochemical analysis of proteins recruited to the site of damage. PCR analysis across the HO recognition site confirms that cleavage is efficient in wild-type cells, attaining $>$90% by 2 hr (Figure 3A).

To assess the presence of the INO80 complex at the HO-induced DSB, we used quantitative real-time PCR analysis on DNA recovered by ChIP in strains carrying fully functional Myc-tagged copies of either Ino80, Arp5, or Arp8. The relative enrichment here is normalized to an uncut locus and a nonspecific antibody ChIP so that any enrichment is obligatorily HO cut- and Myc epitope-specific (see Experimental Procedures). We find that Ino80, Arp5, and Arp8 are all recruited near the HO-induced DSB. Significant recruitment to sites at 0.4 kb (HO2) and 1.6 kb (HO1) from the cleavage consensus can be detected as early as 1 hr after HO induction, reaching a maximum at 4 hr after the switch to galactose (Ino80, $\sim$4-fold at HO1 and $\sim$3.5-fold at HO2; Arp5, $\sim$4.5-fold at HO1 and $\sim$4-fold at HO2; Arp8, $\sim$8-fold at HO1 and $\sim$6-fold at HO2; Figures 3B–3D). Ino80 and Arp5 are recovered with nearly equal efficiency at both HO1 and HO2, while Arp8 shows a slightly higher recovery. This variation among the subunits is slight, however, and can be attributed to operational parameters, such as the efficiency of crosslinking and the stability of the epitope tag during the ChIP procedure. The reproducible and specific increase in the presence of three components of INO80 argues strongly that a functional remodeling complex is recruited to sites near the DSB.

Shroff et al. (2004).
(F) Ino80 recruitment to the DSB at *MAT* requires phosphorylation of histone H2A. Relative fold enrichment at HO1 and HO2 0 and 4 hr after HO induction in the wild-type and *hta1/2*^{S129*} double mutant are compared. The efficiency of DSB induction in wild-type and the H2A mutants was not completely identical, and therefore, the signal for Ino80 enrichment was normalized to the efficiency of DSB induction.

H2A-S129 Phosphorylation Is Required for Ino80 Recruitment

The HO-cut system has been used extensively to demonstrate that HR (*RAD52* epistasis group), NHEJ (*KU*-dependent pathway), and checkpoint proteins (e.g., Mec1) are recruited to the DSB at *MAT* (Kondo et al., 2001; Martin et al., 1999; Sugawara et al., 2003; Wolner et al., 2003). Our data suggest that INO80 may act in concert with such proteins to facilitate DSB repair. One of the early events in mammals in response to the induction of DNA damage is the rapid phosphorylation of histone H2AX adjacent to the site of damage (Fernandez-Capetillo et al., 2004). Phosphorylated H2AX, referred to as γ-H2AX, forms foci that appear to be a prerequisite for repair: the absence of γ-H2AX foci correlates with impaired formation of repair foci at sites of damage (Fernandez-Capetillo et al., 2004). Yeast has no H2A variant identical to the mammalian H2AX, but expresses histone H2A from two genes, *HTA1* and *HTA2* (Redon et al., 2002), which both carry the target serine129 characteristic of H2AX located four residues from the carboxyl terminus. Upon induction of DNA damage, both H2A products become phosphorylated at this conserved serine residue in a manner dependent on the ATM- and ATR-related kinase (Downs et al., 2000; Nakamura et al., 2004). Thus, H2AX in mammals and H2A in yeast both incur rapid modification in response to DNA damage. This raises the question whether H2A phosphorylation in yeast also recruits checkpoint and/or repair proteins, including INO80, to DSB sites.

To address this question, we first examined whether yeast H2A becomes phosphorylated adjacent to the DSB induced at *MAT*. Using a phospho-specific H2A antibody in the same ChIP protocol, we find that H2A is phosphorylated as early as 30 min after induction of HO (4.5-fold enrichment at HO1 and 1.5-fold enrichment at HO2; Figure 3E and data not shown). At the time of maximal cut efficiency (i.e., 2 hr) phosphorylated H2A is still recovered near the cut site (Figure 3E). Both yeast ATM-related kinases Mec1 and Tel1 appear to be required for H2A phosphorylation (Downs et al., 2000; Shroff et al., 2004), and both can be detected at sites of HO-induced damage (Kondo et al., 2001; Nakada et al., 2003). Consistent with the findings of Shroff et al. (2004), we show that the H2A phosphorylation level is reduced but not eliminated in a *mec1* mutant, while it is unaffected in either the *ino80*, *arp5*, or *arp8* deletion backgrounds (data not shown).

To test whether H2A phosphorylation is required for the recruitment of Ino80 to nucleosomes near the DSB, we mutated the H2A target of DNA damage-induced phosphorylation, replacing serine 129 with a stop codon at both *HTA* loci. Upon damage induction, this mutated form is no longer an ATM/ATR kinase target, as confirmed by Western blotting with the S^{129}-phospho-specific H2A antibody (data not shown). The double *hta1/2*^{S129*} mutation was combined with the Myc-tagged Ino80 protein to allow us to monitor Ino80 recruitment upon induction of the HO-dependent DSB. Indeed, the recruitment of Ino80 was significantly reduced in the H2A mutant strain (70% reduced at HO1, 55% reduced at HO2; Figure 3F). Because HO-cleavage efficiency was slightly reduced in the mutant (78% versus 98% in the wild-type at 4 hr), the ChIP signal for Ino80 enrichment has been normalized to cleavage efficiency in these experiments. Thus, the percentages reported reflect a true reduction in bound Ino80 and not the combined effects of impaired cut efficiency and inefficient recruitment. In contrast, we saw no drop in Ino80 recruitment to the DSB in strains deficient for yKu70 or for the checkpoint kinase Rad53 (data not shown). Taken together, our results suggest that phosphorylation of histone H2A is a critical step in the recruitment of Ino80 to sites near a DSB in vivo. The recruitment of INO80 by H2A phosphorylation is likely to be physiologically significant, because mutations in the H2A phospho-acceptor site (Downs et al., 2000) and the INO80 complex (Figure 2) both impair NHEJ efficiency. These results, together with those of Morrison et al. (2004 [this issue of *Cell*]), provide the first demonstration of a link between the recruitment of an ATP-dependent chromatin remodeling complex and histone phosphorylation.

A Mutated INO80 Complex Affects Processing of the DSB

Single-stranded DNA (ssDNA) is a common intermediate found at sites of DNA damage. In yeast, ssDNA has been found at the HO DSB, where it functions not only to initiate DNA repair, but also to activate an efficient and sustained checkpoint response (Lee et al., 1998; Vaze et al., 2002; Wang and Haber, 2004). A prerequisite for ssDNA formation is that an exonuclease gains access to the damaged DNA, which might well be embedded in condensed chromatin. We reasoned that chromatin remodeling by INO80 could facilitate access for exonucleases to a damaged site. The outcome would be that INO80 facilitates ssDNA formation.

To test this hypothesis we determined the amount of ssDNA formed at the HO DSB in wild-type, *arp8*, and *hta1/2*^{S129*} strains. We chose the *arp8* strain because the loss of Arp8 severely compromises the INO80 chromatin remodeling activity (Shen et al., 2003) and chose the *hta1/2*^{S129*} strain as it is defective for Ino80 recruitment to the break (Figure 3F). An *INO80* disruption could not be tested as it is lethal in the Gal-HO background. To monitor the formation of ssDNA at the DSB in the absence and presence of INO80-dependent chromatin remodeling, we adapted a PCR-based method called quantitative amplification of ssDNA (QAOS) developed by Booth et al. (2001).

The use of nested primers on a nondenatured template during the first round of amplification (Figure 4A) allows a quantitative evaluation of the amount of ssDNA present at the HO1 primer site near the DSB. Because the efficiency of galactose-induced cleavage drops slightly in both the *arp8* and *hta1/2*^{S129*} mutants (Figure 4B, % DSB), we again normalized the amount of ssDNA detected by QAOS to the cleavage efficiency. Single-stranded template can be detected as early as 1 hr after DSB induction in wild-type and mutant cells, and its level increases to about 85% of the available template by 4 hr in the wild-type strain. In both the *arp8* and *hta1/2*^{S129*}, mutants we note a significant reduction in ssDNA after 2 to 4 hr on galactose, with values less than half of the amount recovered in wild-type cells (Figure 4B). Consistent with this drop in ssDNA, we also detect a significant reduction (85% to 90%) in the recruitment

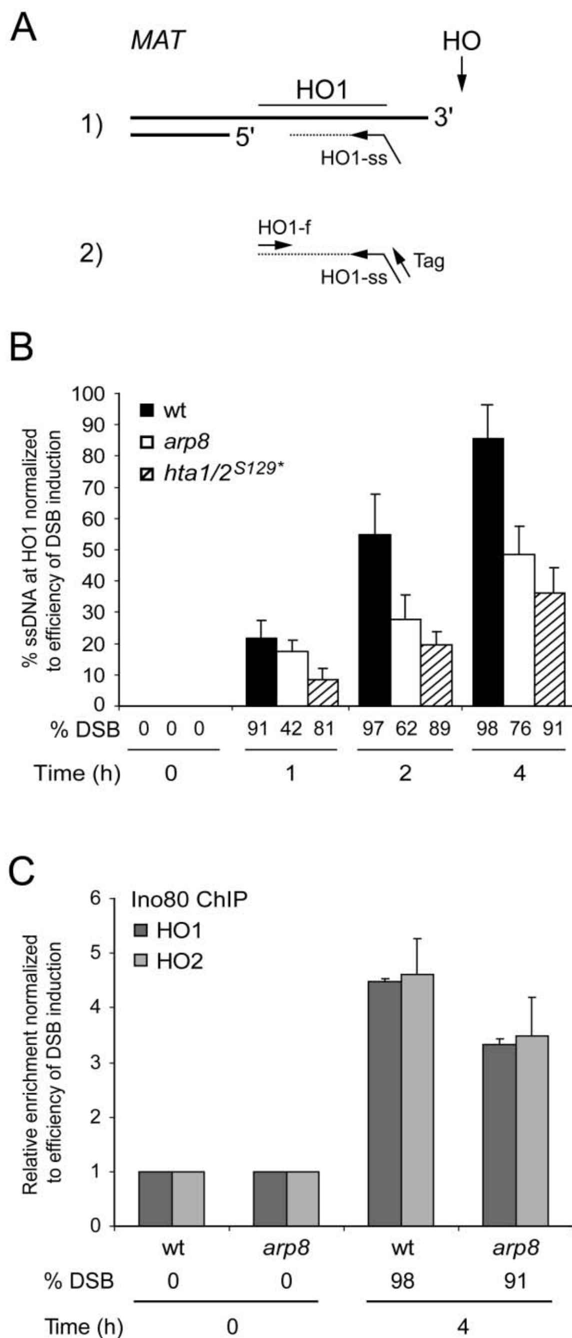

Figure 4. Formation of ssDNA at the DSB Is Reduced in *arp8* and *hta1/2*^{S129*} Mutants

(A) Schematic representation of the QAOS (quantitative amplification of single-stranded DNA) method used to amplify ssDNA at the HO1 site near the DSB at *MAT*. At low temperatures the HO1-ss primer recognizes and binds to ssDNA within the HO1 region (1.6 kb away from the DSB), and a round of primer extension without denaturation creates a novel template molecule from the ssDNA template (1). This novel template molecule is quantified by real-time PCR using primers HO1-f and Tag (2).

(B) Reduced ssDNA at the DSB in *arp8* and *hta1/2*^{S129*} mutants. The amount of ssDNA formed at the HO1 site 0, 1, 2, and 4 hr after HO induction in wild-type (black bars), *arp8* (white bars), and *hta1/2*^{S129*} (hatched bars) strains was determined by QAOS. The amount of ssDNA is corrected for the efficiency of strand cleavage in wild-type, *arp8*, and *hta1/2*^{S129*} strains, respectively.

(C) Ino80 recruitment to the DSB at *MAT* is slightly impaired in an *arp8* mutant. Relative fold enrichment at HO1 and HO2 are compared at 0 and 4 hr after HO induction in wild-type and *arp8* cells. The signal for Ino80 enrichment was normalized to the efficiency of DSB induction.

of the Mec1/Ddc2 complex to the processed break in the *arp8* mutant (data not shown), an event that is dependent on the ssDNA binding complex RPA (Zou and Elledge, 2003; K. Dubrana, H.v.A., and S.M.G., unpublished data).

The inefficient conversion of dsDNA to ssDNA in strains lacking INO80 activity at the DSB could either reflect an absence of nucleosome remodeling or loss of the INO80-associated 3′ to 5′ helicase activity. In the *arp8* strain, the large Ino80 subunit is present in an INO80 subcomplex which retains the two helicase subunits, Rvb1 and Rvb2, yet is nonfunctional for remodeling nucleosomes (Shen et al., 2003). We next monitored whether this residual INO80 subcomplex is recruited to the DSB by performing ChIP for Ino80 itself in the *arp8* mutant. As shown in Figure 4C, Ino80 is indeed recruited, albeit at about 75% of wild-type levels. These data are consistent with data from Morrison et al. (2004), which show that the Nhp10 subunit is responsible for the interaction between INO80 and phosphorylated H2A at a DSB. In the *arp8* mutant, we monitor a drop in ssDNA formation (Figure 4B) and a hypersensitivity to DSB formation (Figure 2C), coincident with the recruitment of the remodeling-deficient INO80 subcomplex, suggesting that chromatin remodeling is indeed necessary for efficient processing of the DSB. While we do not rule out a contribution of the Rvb subunits, our data indicate that the Rvb helicase activity cannot be sufficient to account for the impact INO80 recruitment has on DSB processing. Our data argue therefore that the remodeling activity of INO80 on nucleosomes near the DSB facilitates DNA end processing and subsequent repair.

Discussion

Although the role of ATP-dependent chromatin remodeling complexes in transcription has been reasonably well established, defining their roles in processes other than transcription has remained elusive. Here, we implicate the ATP-dependent INO80 nucleosome remodeling complex in the repair of DNA damage. As demonstrated for the mammalian H2A variant H2AX, yeast histone H2A becomes rapidly phosphorylated near sites of chromosomal damage (Downs et al., 2000; Fernandez-Capetillo et al., 2004). The modification is mediated by ATR and ATM kinases in both yeast and man (Fernandez-Capetillo et al., 2004; Nakamura et al., 2004; Shroff et al., 2004). By mutating the phosphoacceptor site, and monitoring INO80 recruitment to the site of damage, we show causality between histone modification and the recruitment of a remodeling complex to nucleosomes near the DSB. In parallel, Morrison et al. (2004) have demonstrated that the INO80 complex can directly bind the phosphorylated form of H2A through its small HMG-like subunit, Nhp10. Recruitment is dependent on the action of Tel1 and Mec1 kinases, presumably reflecting their

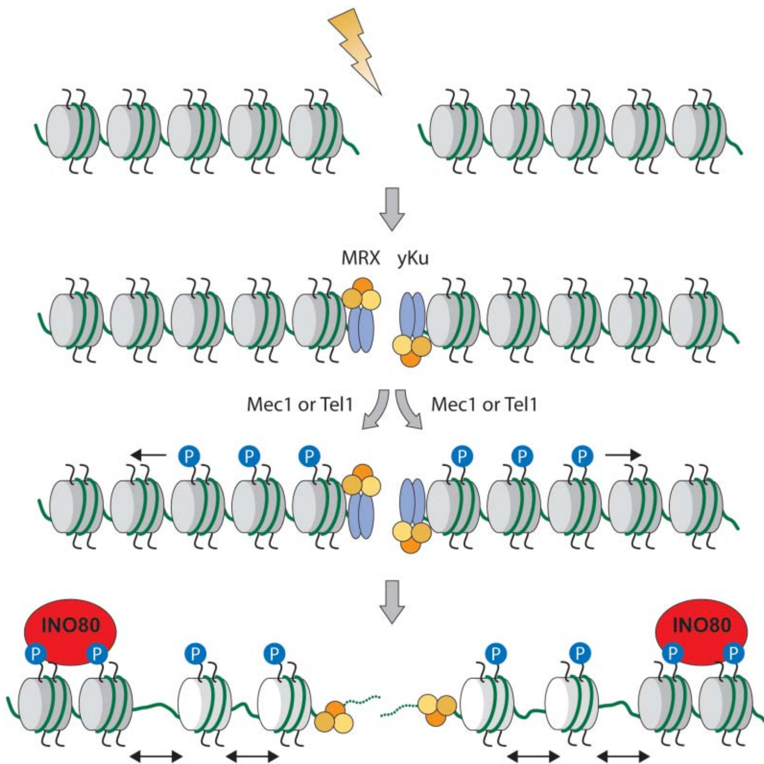

Figure 5. Model for the Events Leading to the Recruitment of INO80 to a DSB and Its Role in Lesion Processing

Schematic proposal for the events leading to the recruitment of INO80 to sites near a DSB, and its role in processing of this lesion. As described in the text, cleaved ends are rapidly bound by yKu and the Mre11/Rad50/Xrs2 complex (MRX), which may help recruit the ATM kinase Tel1. H2A Ser129 phosphorylation is achieved by either Tel1 and/or Mec1, creating a recognition site for the Nhp10 subunit of INO80 (Morrison et al., 2004). The INO80 remodeler could then alter histone position facilitating conversion to ssDNA (dashed green line) by either MRX, Exo1, or other enzymes. Alternatively, INO80 itself may contribute to helix unwinding. It is unclear whether INO80 spreads with phosphorylated H2A or remains localized at the break through other protein interactions.

role in the modification of H2A. This proposed role for ATM-related kinases reinforces our finding that there is a drop in Ino80 recruitment in the H2A phosphoacceptor site mutant (*hta1/2*^{S129*}). We conclude that if serine 129 of H2A fails to be phosphorylated, either due to the absence of ATM/ATR kinases or due to mutation of the acceptor site, then the INO80 complex is unable to specifically recognize the damaged locus and fails to be recruited.

Why Recruit INO80 to a Double-Strand Break?

We show here that *INO80*-, *ARP5*-, and *ARP8*-deficient cells are hypersensitive to DNA-damaging agents that produce breaks repaired by either HR (i.e., MMS) or NHEJ (i.e., at HO-induced cuts). While the drug sensitivity of *ino80* mutants may be aggravated by the misregulation of genes involved in repair or cell cycle control, the observed drop in *DNL4* expression per se is unlikely to account for the MMS and HU sensitivity found in the *arp5* and *arp8* mutant strains. In support of a transcription-independent role for INO80 at DSBs, others have shown that the elimination of serine 129 in yeast H2A leads to impaired NHEJ (Downs et al., 2000) and to deficiencies in DSB repair during replication (Redon et al., 2003). It has been further established in mice that H2AX is required for both HR and NHEJ repair (Fernandez-Capetillo et al., 2004). The quantitative ChIP shown here for three different subunits of the INO80 complex and our analysis of ssDNA at the DSB in wild-type, *arp8*, and *hta1/2*^{S129*} strains argue that the recruitment of the intact yeast INO80 complex to sites of damage promotes remodeling events, which in turn facilitate access for proteins involved in resection of the break site. The production of a 3′ overhang occurs during HR as well as during error-prone, microhomology-dependent NHEJ (Moore and Haber, 1996), and thus INO80 may be important for multiple pathways of DSB repair.

The conservation of the INO80 complex (Bakshi et al., 2004) and of DSB-induced phosphorylation of the histone H2A C-terminal domain suggests that the INO80-γ-H2AX interaction will be important in other organisms. While it is well established that γ-H2AX influences repair of DSBs in mammalian cells (Fernandez-Capetillo et al., 2004), it is not known whether loss of mammalian Ino80 impairs the cellular response to DNA damage. Recent work in *Arabidopsis* shows that a mutant affected in the expression of the *Arabidopsis* Ino80 ortholog (AtIno80) is specifically defective for HR (Fritsch et al., 2004). In the same study it was shown that transcriptional regulation of DNA repair genes was not significantly affected by mutations in AtIno80, suggesting that the presumed *Arabidopsis* INO80 complex, like the yeast counterpart, plays a direct role in facilitating repair. It remains to be seen, however, whether γ-H2AX recruits AtIno80 to damage.

The Stability of a Break: A Matter of Nucleosomes?

In budding yeast the HO-induced DSB is remarkably stable, with a half-life of nearly 1 hr under conditions that eliminate ligation (Frank-Vaillant and Marcand, 2002). These authors showed that the stable end is necessary for efficient and error-free NHEJ, and that NHEJ precedes HR in normal haploid cells. In other words, the 5′ to 3′ resection necessary for strand invasion during HR seemed to occur only once NHEJ had failed. The

Table 1. Yeast Strains Used in This Study

Strain	Genotype	Reference
BY4733	*MATa his3-200 leu2 met15 trp1-63 ura3*	Research Genetics
GA-2264	BY4733 *ino80::TRP1*	(Shen et al., 2000)
GA-2369	BY4733 *yku70::natMX4*	This study
7375	*MATa arp5::kanMX4 his3-1 leu2 met15 ura3*	Research Genetics
2397	*MATa arp8::kanMX4 his3-1 leu2 met15 ura3*	Research Genetics
JKM179	*MATα ade1 leu2-*3,*112 lys5 trp1::hisG ura3*-52 *hml::ADE1 hmr::ADE1 ade3::GALHO*	(Lee et al., 1998)
GA-2315	JKM179 *arp5::kanMX4*	This study
GA-2316	JKM179 *arp8::kanMX4*	This study
GA-3011	JKM179 *yku70::LEU2*	This study
GA-2309	JKM179 *INO80-myc(::kanMX4)*	This study
GA-2317	JKM179 *ARP5-myc(::kanMX)*	This study
GA-2318	JKM179 *ARP8-myc(::kanMX)*	This study
GA-2824	JKM179 *INO80-myc(::kanMX4) hta1S129* hta2S129**	This study
GA-2311	JKM179 *INO80-myc(::kanMX4) arp8::natMX4*	This study

Note that the first five strains are in the S288C background, which tolerates *ino80* deletion, while all others are derivatives of JKM179 (Lee et al., 1998), which, like W303, does not survive upon *ino80* deletion.

delay in processing could reflect a barrier imposed by the nucleosomes that flank the DSB in vivo, or else indicate that the recruitment of exonucleases and other processing enzymes is slow. We show here that the appearance of a 3′ single-strand overhang occurs even more slowly in strains that either fail to recruit INO80 to the DSB (i.e., *hta1/2*^{S129*}; Figure 3F) or recruit a remodeling-deficient INO80 complex (i.e., *arp8*; Figure 4C). Our results argue that the association of a remodeling competent INO80 complex facilitates exonuclease action at the DSB. The appearance of ssDNA is consistent with the kinetics of recruitment that we monitor for the INO80 complex. On the other hand, INO80 does not seem to be necessary for the binding of yKu or MRX, as these complexes associate far more rapidly with DSBs than INO80 (Martin et al., 1999; Frank-Vaillant and Marcand, 2002; Shroff et al., 2004).

A proposed chronology of protein recruitment and modifications at DSBs is shown in Figure 5. MRX and yKu appear to be the first proteins recruited to breaks, and neither factor spreads far from the cleavage site (Martin et al., 1999; Shroff et al., 2004). The MRX complex may help hold DNA ends together and targets the checkpoint kinase Tel1, or in its absence perhaps Mec1, to the lesion. At this point H2A tails become phosphorylated on residue S129, which provides a binding site for INO80. The fact that all three subunits of INO80, i.e., Ino80, Arp5, and Arp8, are recruited with similar kinetics suggests that they bind as a complex and not as individual components (Figure 5). Further support for this model is the observation that elimination of the H2A phosphorylation site severely reduces Ino80 binding. Finally, INO80 facilitates, through its chromatin remodeling activity, the conversion of the DSB to a 3′ ssDNA overhang.

Our data suggest that H2A phosphorylation is necessary for INO80 recruitment. Histone acetylation and deacetylation also seem to be essential components of the cellular pathway for DSB repair (Bird et al., 2002; Downs et al., 2000; Jazayeri et al., 2004), yet it is not known whether they contribute to the signal for INO80 recruitment. Multiple histone tail modifications may form a composite signal, and further studies are needed to show if H2A phosphorylation is sufficient for INO80 recruitment. We speculate that at later time points INO80 may bind near the DSB through a mechanism different from recognition of phosphorylated H2A (Morrison et al., 2004), since the kinetics of INO80 binding near the cut site are different from those reported for H2AX (Shroff et al., 2004). It is plausible that histone acetylation/deacetylation or other protein-protein interactions could help stabilize chromatin modifying enzymes at the break. In this context we note that the INO80 component Rvb1 is reported to interact with both yKu and RFA (Ho et al., 2002).

Does INO80 Have Other Functions at the DSB?

In the absence of INO80 recruitment we detect less ssDNA at an unrepaired cleavage site. It is possible that the resection, which is thought to be mediated either by the MRX complex (Lee et al., 1998), by Exo1, or other nucleases, is aided directly by the 3′ to 5′ helicase activity of the INO80 complex (Shen et al., 2000). *Arp8* mutants recruit a remodeling-defective INO80 complex and have impaired end processing (Figure 4B). Since the Arp8-deficient INO80 complex retains Rvb1 and Rvb2 (Shen et al., 2003), it will be of interest to assay whether this residual complex maintains helicase activity. If not, specific separation of function mutants in the Rvb1/2 subunits will be necessary to test whether or not INO80 contributes to DSB processing through its helicase activity, as well as through nucleosome remodeling. The intriguing coordination of nucleosome remodeling events for gene expression (e.g., *DNL4)* and for DNA repair suggests that yeast may guarantee a particular response to DNA damage by implicating the INO80 complex in both mechanisms.

Experimental Procedures

Yeast Strains

Yeast strains are listed in Table 1. All yeast strains were grown at 30°C on rich YPAD or selective Synthetic Complete medium unless otherwise indicated. Complete null and Myc-tagged alleles (except for the Myc-*Mec1* allele; Paciotti et al., 2000) were made by standard PCR-based gene disruption and insertion methods (Wach et al., 1994; Goldstein and McCusker, 1999). All deletions and insertions were verified by PCR, and expression and complementation of Myc-

tagged proteins was verified by Western blot analysis and MMS sensitivity assays. The GA-2824 strain which carries the *hta1S129** *hta2S129** mutations was made by site-directed mutagenesis of the codon for Ser129 to a stop codon (S129*). A PCR fragment containing the *hta1S129** mutation and a *loxP-URA3(K. lactis)-loxP* cassette was amplified by PCR using pUG72 (Gueldener et al., 2002) and introduced into the histone *HTA1* gene in GA-2309. After verification of the insertion and counterselection on medium containing 5-FOA, the procedure was repeated for the *HTA2* gene to introduce the *hta2S129** mutation, producing GA-2824. Western blot analysis of MMS treated GA-2309 and GA-2824 cells with a phosphospecific H2A polyclonal antibody (gift from W. Bonner, NIH, Bethesda, Maryland) detected phosphorylated H2A in GA-2309, but not in GA-2824 (data not shown).

DNA Damage Survival Assays

BY4733 (wt), GA-2264 (*ino80*), 7375 (*arp5*), 2397 (*arp8*), and GA-2369 (*yku70*) cells were grown on YPAD. Purified colonies were resuspended in water and 10-fold serial dilutions were spotted on YPAD, YPAD containing 0.03% MMS (Sigma), and YPAD containing 100 mM HU (US Biologicals). Images of the colonies were taken after 4–5 days at 30°C.

Cells containing the galactose-inducible HO endonuclease were grown overnight to 5×10^6 cells/ml in medium containing 3% glycerol, 2% lactic acid, and 0.05% glucose. After washing once with water, aliquots of 10-fold serial dilutions were plated on rich medium containing 3% glycerol and 2% lactic acid, supplemented with either 2% galactose or 2% glucose. Colonies were counted 3–5 days after plating. Survival efficiency is colonies formed on galactose divided by colonies formed on glucose.

Plasmid pCM190-HO, which contains the *HO* gene under control of a doxycycline-regulatable promoter, was constructed by cloning the *HO* gene from pGAL-HO into PmeI-digested pCM190 (Gari et al., 1997). pCM190 was transformed into GA-1081 (wt), GA-2315 (*arp5*), GA-2316 (*arp8*), and GA-3011 (*yku70*). After transformation, cells were grown on selective medium containing 10 μg/ml doxycycline (Sigma) in order to tightly repress HO expression. Sensitivity to the doxycycline-regulated HO-mediated cleavage was assayed by spotting 10-fold serial dilutions on selective medium with and without 10 μg/ml doxycycline. Colonies were imaged after 5–7 days at 30°C.

Western Blot Analysis of Rad53

Protein extracts were prepared from rapidly growing cultures treated 2 hr with or without 0.05% MMS and analyzed on 7% SDS polylacrylamide gels. Rad53 was detected by sequential incubations with polyclonal goat anti-Rad53 antibody (Santa Cruz), horseradish peroxidase conjugated rabbit anti-goat antibody (Sigma), and the Enhanced Chemi-Luminescence system (Amersham).

Transcriptome Analysis

The transcriptomes of *ino80* (GA-2264) and *arp8* (2397) mutant cells were compared to that of wild-type cells (BY4733) after 1h at 30°C in the absence or presence of 0.1% MMS. All conditions were profiled from duplicates obtained from two independent experiments.

For the analysis of untreated and MMS-treated *ino80* or *arp8* cells, the list of potentially modulated genes was submitted to a one-way ANOVA test (variances considered as equal, p value of 0.05) for changes between the four conditions (wt, wt MMS-treated, *ino80*, *ino80* MMS-treated cells) and a post-hoc Turkey test, resulting in lists of genes that display significant changes in their steady-state expression in wild-type and *ino80*, wild-type and wild-type MMS-treated, and *ino80* and *ino80* MMS-treated cells. The same procedure was applied for the *arp8* analysis (Supplemental Tables S1, S2, and S3 on the *Cell* website). A custom list of 702 repair, cell cycle, and DNA processing genes was constructed, and those showing MMS regulation in wild-type and/or *ino80* cells were further filtered for fold changes >1.5. The resulting list (Supplemental Table S4 on the *Cell* website) was also analyzed for changes relative to the *arp8* mutation. Details of the analysis are found in Supplemental Data on the *Cell* website.

ChIP and QAOS at the HO DSB

Chromatin immunoprecipitation was performed basically as described (Martin et al., 1999) on the indicated strains, except that 2% galactose was added to induce the HO endonuclease, or 2% glucose to repress it, after growth to $1–5 \times 10^6$ cells/ml in rich media containing 3% glycerol, 2% lactic acid, and 0.05% glucose. Details of ChIP are available in the Supplemental Data on the *Cell* website. For quantitation, signals from near the DSB (HO1 and HO2) are normalized to a control signal from a noncut region in *SMC2*. The signals are also normalized to the input signal for each primer set at each time point, since end processing can reduce the available DNA complement. Finally, at each time point a nonimmune antibody control (anti-HA) is used as a background, against which all values are normalized. ChIP data are presented as the mean of multiple experiments ± SD.

The efficiency of DSB induction was determined by PCR on input DNA. Primer SG442 (5′-AGT ATG CTG GAT TTA AAC TCA TCT GTG ATT TGT GG-3′) and SG443 (5′-TCCGTCCCGTATAGCCAATTC GTTC-3′), which span the HO recognition site, were used in combination with primer SG444 (5′-GACGACCTTGTAACAGTCCAGACAG-3′) and SG135 (5′-GGCGAATTCCATCACATTATAC TAACTACGG-3′), which anneal to the *SMC2* control locus. PCR products were separated by agorose gel electrophoresis, and signal intensities were determined using a Biorad Fluor-S multi-imager in combination with Quantity One software. The efficiency of DSB induction was calculated as ratio of the HO/SMC signal of induced cells normalized to that of uninduced cells.

ssDNA at the HO-induced DSB was measured by the real-time quantitative PCR-based method termed QAOS (quantitative amplification of ssDNA; Booth et al., 2001). We calculated ssDNA percentages based on total denatured HO1 signal for each time point and sample because the global amount of HO1 sequence decreases over time. A standard curve was made as described (Booth et al., 2001) to verify the accuracy and quantification of ssDNA detection (K. Dubrana, H.v.A., and S.M.G., unpublished data). Primers HO1-ss (5′-ATCTCGAGCGTCATATCGGATCACACAAT TCATAAGTC-3′), HO1-f (SG573), and Tag (5′-ATCTCGAGCGTCATATCGGATCAC-3′) were used for QAOS in combination with the HO1 probe as indicated in Figure 4A. QAOS data are presented as the mean of multiple experiments ±SD.

Acknowledgments

The Gasser laboratory acknowledges the Swiss Cancer League, the Swiss National Science Foundation, European RTN Checkpoints and Cancer, and fellowships from EMBO and Human Frontiers Science Program to H.v.A. B.H., and O.F. acknowledge support from the Novartis Foundation. We thank colleagues in the Gasser laboratory for helpful discussions, Ed Oakeley (FMI, Basel) for excellent microarray advice, William Bonner for H2A-P antibody, Jim Haber and Xuetong Shen for strains, and Nicolas Roggli for excellent artistic support. We further thank Xuetong Shen and Alan Tomkinson for communicating results prior to publication and Alessandro Bianchi, Florence Hediger, Kenji Shimada, and Thomas Schleker for critically reading the manuscript.

Received: August 17, 2004
Revised: November 1, 2004
Accepted: November 11, 2004
Published: December 16, 2004

References

Bakshi, R., Prakash, T., Dash, D., and Brahmachari, V. (2004). In silico characterization of the INO80 subfamily of SWI2/SNF2 chromatin remodeling proteins. Biochem. Biophys. Res. Commun. *320*, 197–204.

Bird, A.W., Yu, D.Y., Pray-Grant, M.G., Qiu, Q., Harmon, K.E., Megee, P.C., Grant, P.A., Smith, M.M., and Christman, M.F. (2002). Acetylation of histone H4 by Esa1 is required for DNA double-strand break repair. Nature *419*, 411–415.

Booth, C., Griffith, E., Brady, G., and Lydall, D. (2001). Quantitative amplification of single-stranded DNA (QAOS) demonstrates that

cdc13–1 mutants generate ssDNA in a telomere to centromere direction. Nucleic Acids Res. *29*, 4414–4422.

Downs, J.A., Lowndes, N.F., and Jackson, S.P. (2000). A role for Saccharomyces cerevisiae histone H2A in DNA repair. Nature *408*, 1001–1004.

Ebbert, R., Birkmann, A., and Schuller, H.J. (1999). The product of the SNF2/SWI2 paralogue INO80 of Saccharomyces cerevisiae required for efficient expression of various yeast structural genes is part of a high-molecular-weight protein complex. Mol. Microbiol. *32*, 741–751.

Fernandez-Capetillo, O., Lee, A., Nussenzweig, M., and Nussenzweig, A. (2004). H2AX: the histone guardian of the genome. DNA Repair (Amst.) *3*, 959–967.

Foss, E.J. (2001). Tof1p regulates DNA damage responses during S phase in Saccharomyces cerevisiae. Genetics *157*, 567–577.

Frank-Vaillant, M., and Marcand, S. (2001). NHEJ regulation by mating type is exercised through a novel protein, Lif2p, essential to the ligase IV pathway. Genes Dev. *15*, 3005–3012.

Frank-Vaillant, M., and Marcand, S. (2002). Transient stability of DNA ends allows nonhomologous end joining to precede homologous recombination. Mol Cell. *5*, 1189–1199.

Fritsch, O., Benvenuto, G., Bowler, C., Molinier, J., and Hohn, B. (2004). The INO80 protein controls homologous recombination in *Arabidopsis thaliana*. Mol. Cell *16*, 479–485.

Gari, E., Piedrafita, L., Aldea, M., and Herrero, E. (1997). A set of vectors with a tetracycline-regulatable promoter system for modulated gene expression in S. cerevisiae. Yeast *13*, 837–848.

Goldstein, A.L., and McCusker, J.H. (1999). Three new dominant drug resistance cassettes for gene disruption in S. cerevisiae. Yeast *15*, 1541–1553.

Gueldener, U., Heinisch, J., Koehler, G.J., Voss, D., and Hegemann, J.H. (2002). A second set of loxP marker cassettes for Cre-mediated multiple gene knockouts in budding yeast. Nucleic Acids Res. *30*, e23.

Harata, M., Oma, Y., Mizuno, S., Jiang, Y.W., Stillman, D.J., and Wintersberger, U. (1999). The nuclear actin-related protein of S. cerevisiae, Act3p/Arp4, interacts with core histones. Mol. Biol. Cell *10*, 2595–2605.

Ho, Y., Gruhler, A., Heilbut, A., Bader, G.D., Moore, L., Adams, S.L., Millar, A., Taylor, P., Bennett, K., Boutilier, K., et al. (2002). Systematic identification of protein complexes in S. cerevisiae by mass spectrometry. Nature *415*, 180–183.

Jaskelioff, M., Van Komen, S., Krebs, J.E., Sung, P., and Peterson, C.L. (2003). Rad54p is a chromatin remodelling enzyme required for heteroduplex DNA joint formation with chromatin. J. Biol. Chem. *278*, 9212–9218.

Jazayeri, A., McAinsh, A.D., and Jackson, S.P. (2004). Saccharomyces cerevisiae Sin3p facilitates DNA double-strand break repair. Proc. Natl. Acad. Sci. USA *101*, 1644–1649.

Jelinsky, S.A., and Samson, L.D. (1999). Global response of Saccharomyces cerevisiae to an alkylating agent. Proc. Natl. Acad. Sci. USA *96*, 1486–1491.

Katou, Y., Kanoh, Y., Bando, M., Noguchi, H., Tanaka, H., Ashikari, T., Sugimoto, K., and Shirahige, K. (2003). S-phase checkpoint proteins Tof1 and Mrc1 form a stable replication-pausing complex. Nature *424*, 1078–1083.

Kegel, A., Sjostrand, J.O., and Astrom, S.U. (2001). Nej1p, a cell type-specific regulator of nonhomologous end joining in yeast. Curr. Biol. *11*, 1611–1617.

Kondo, T., Wakayama, T., Naiki, T., Matsumoto, K., and Sugimoto, K. (2001). Recruitment of Mec1 and Ddc1 checkpoint proteins to double-strand breaks through distinct mechanisms. Science *294*, 867–870.

Lee, S.E., Moore, J.K., Holmes, A., Umezu, K., Kolodner, R.D., and Haber, J.E. (1998). *Saccharomyces* Ku70, mre11/rad50, and RPA proteins regulate adaptation to G2/M arrest after DNA damage. Cell *94*, 399–409.

Lusser, A., and Kadonaga, J.T. (2003). Chromatin remodeling by ATP-dependent molecular machines. Bioessays *25*, 1192–1200.

Martin, S.G., Laroche, T., Suka, N., Grunstein, M., and Gasser, S.M. (1999). Relocalization of telomeric Ku and SIR proteins in response to DNA strand breaks in yeast. Cell *97*, 621–633.

Melo, J., and Toczyski, D. (2002). A unified view of the DNA-damage checkpoint. Curr. Opin. Cell Biol. *14*, 237–245.

Mizuguchi, G., Shen, X., Landry, J., Wu, W.H., Sen, S., and Wu, C. (2004). ATP-driven exchange of histone H2AZ variant catalyzed by SWR1 chromatin remodelling complex. Science *303*, 343–348.

Moore, J.K., and Haber, J.E. (1996). Cell cycle and genetic requirements of two pathways of nonhomologous end-joining repair of double-strand breaks in S. cerevisiae. Mol. Cell. Biol. *16*, 2164–2173.

Morrison, A.J., Highland, J., Krogan, N.J., Arbel-Eden, A., Greenblatt, J.F., Haber, J.E., and Shen, X. (2004). INO80 and γ-H2AX interaction links ATP-dependent chromatin remodeling to DNA damage repair. Cell *119*, this issue, 767–775.

Nakada, D., Matsumoto, K., and Sugimoto, K. (2003). ATM-related Tel1 associates with double-strand breaks through an Xrs2-dependent mechanism. Genes Dev. *17*, 1957–1962.

Nakamura, T.M., Du, L.-L., Redon, C., and Russell, P. (2004). Histone H2A phosphorylation controls Crb2 recruitment at DNA breaks, maintains checkpoint arrest, and influences DNA repair in fission yeast. Mol. Cell. Biol. *24*, 6215–6230.

Paciotti, V., Clerici, M., Lucchini, G., and Longhese, M.P. (2000). The checkpoint protein Ddc2, functionally related to S. pombe Rad26, interacts with Mec1 and is regulated by Mec1-dependent phosphorylation in budding yeast. Genes Dev. *14*, 2046–2059.

Peterson, C.L., and Cote, J. (2004). Cellular machineries for chromosomal DNA repair. Genes Dev. *18*, 602–616.

Petukhova, G., Stratton, S., and Sung, P. (1998). Catalysis of homologous DNA pairing by yeast Rad51 and Rad54 proteins. Nature *393*, 91–94.

Reagan, M.S., and Friedberg, E.C. (1997). Recovery of RNA polymerase II synthesis following DNA damage in mutants of Saccharomyces cerevisiae defective in nucleotide excision repair. Nucleic Acids Res., *25*, 4257–4263.

Redon, C., Pilch, D., Rogakou, E., Sedelnikova, O., Newrock, K., and Bonner, W. (2002). Histone H2A variants H2AX and H2AZ. Curr. Opin. Genet. Dev. *12*, 162–169.

Redon, C., Pilch, D.R., Rogakou, E.P., Orr, A.H., Lowndes, N.F., and Bonner, W.M. (2003). Yeast histone 2A serine 129 is essential for the efficient repair of checkpoint-blind DNA damage. EMBO Rep. *4*, 678–684.

Schar, P., Herrmann, G., Daly, G., and Lindahl, T. (1997). A newly identified DNA ligase of S. cerevisiae involved in RAD52-independent repair of DNA double-strand breaks. Genes Dev. *11*, 1912–1924.

Shen, X., Mizuguchi, G., Hamiche, A., and Wu, C. (2000). A chromatin remodelling complex involved in transcription and DNA processing. Nature *406*, 541–544.

Shen, X., Ranallo, R., Choi, E., and Wu, C. (2003). Involvement of actin-related proteins in ATP-dependent chromatin remodeling. Mol. Cell *12*, 147–155.

Shroff, R., Arbel-Eden, A., Pilch, D., Ira, G., Bonner, W.M., Petrini, J.H., Haber, J.E., and Lichten, M. (2004). Distribution and dynamics of chromatin modification induced by a defined DNA double-strand break. Curr. Biol. *14*, 1703–1711.

Sugawara, N., Wang, X., and Haber, J.E. (2003). In vivo roles of Rad52, Rad54, and Rad55 proteins in Rad51-mediated recombination. Mol. Cell *12*, 209–219.

Teo, S.H., and Jackson, S.P. (1997). Identification of S. cerevisiae DNA ligase IV: involvement in DNA double-strand break repair. EMBO J. *16*, 4788–4795.

Valencia, M., Bentele, M., Vaze, M.B., Herrmann, G., Kraus, E., Lee, S.E., Schar, P., and Haber, J.E. (2001). NEJ1 controls non-homologous end joining in S. cerevisiae. Nature *414*, 666–669.

Vaze, M.B., Pellicioli, A., Lee, S.E., Ira, G., Liberi, G., Arbel-Eden, A., Foiani, M., and Haber, J.E. (2002). Recovery from checkpoint-mediated arrest after repair of a double-strand break requires Srs2 helicase. Mol. Cell *10*, 373–385.

Wach, A., Brachat, A., Pohlmann, R., and Philippsen, P. (1994). New heterologous modules for classical or PCR-based gene disruptions in S. cerevisiae. Yeast *10*, 1793–1808.

Wang, X., and Haber, J.E. (2004). Role of Saccharomyces single-stranded DNA-binding protein RPA in the strand invasion step of double-strand break repair. PLoS Biol. 2(1): e21 DOI: 10.1371/journal.pbio.0020021.

Wolner, B., van Komen, S., Sung, P., and Peterson, C.L. (2003). Recruitment of the recombinational repair machinery to a DNA double-strand break in yeast. Mol. Cell *12*, 221–232.

Zhou, B.B., and Elledge, S.J. (2000). The DNA damage response: putting checkpoints in perspective. Nature *408*, 433–439.

Zou, L., and Elledge, S.J. (2003). Sensing DNA damage through ATRIP recognition of RPA-ssDNA complexes. Science *300*, 1542–1548.